Few-Cycle Driven Relativistically Oscillating Plasma Mirrors: A Source of Intense Isolated Attosecond Pulses

P. Heissler,[1,*] R. Hörlein,[1] J. M. Mikhailova,[1,2] L. Waldecker,[1] P. Tzallas,[3] A. Buck,[1,4] K. Schmid,[1] C. M. S. Sears,[1] F. Krausz,[1,4] L. Veisz,[1] M. Zepf,[5] and G. D. Tsakiris[1]

[1]*Max-Planck-Institut für Quantenoptik, D-85748 Garching, Germany*
[2]*A. M. Prokhorov General Physics Institute, Russian Academy of Science, 119991 Moscow, Russia*
[3]*Institute of Electronic Structure and Laser, FORTH, GR-71110 Heraklion (Crete), Greece*
[4]*Fakultät für Physik, Ludwig-Maximilians-Universität München, D-85748 Garching, Germany*
[5]*Department of Physics and Astronomy, Queens University Belfast, BT7 INN, United Kingdom*

(Received 11 January 2012; published 6 June 2012)

The conditions required for the production of isolated attosecond pulses from relativistically oscillating mirrors (ROM) are investigated numerically and experimentally. In simulations, carrier-envelope-phase-stabilized three-cycle pulses are found to be sufficient to produce isolated attosecond pulses, while two-cycle pulses will predominantly lead to isolated attosecond pulses even in the absence of carrier-envelope stabilization. Using a state-of-the-art laser system delivering three-cycle pulses at multiple-terawatt level, we have generated higher harmonics up to 70 eV photon energy via the ROM mechanism. The observed spectra are in agreement with theoretical expectations and highlight the potential of few-cycle-driven ROM harmonics for intense isolated attosecond pulse generation for performing extreme ultraviolet-pump extreme ultraviolet-probe experiments.

DOI: 10.1103/PhysRevLett.108.235003 PACS numbers: 52.59.Ye, 42.65.Ky, 52.38.−r, 52.65.Rr

Recent progress in laser technology [1] has opened the door to the generation of flashes of light that can ''freeze'' the ultrafast motion of electrons in atoms and molecules. The controlled generation of single attosecond (1 as = 10^{-18} s) extreme ultraviolet bursts via harmonic generation in gaseous media [2–5] was promptly followed by an upsurge of fascinating applications [6–8]. Unfortunately, current attosecond sources cannot efficiently exploit state-of-the-art multiple-terawatt and petawatt class laser systems to increase the photon flux. Achieving the ultimate limits of temporal resolution requires attosecond pulses to be used both as the ''trigger'' (or ''pump'') *and* as the ''hyperfast-shutter camera'' (or ''probe'') of the microscopic motion to be studied. This requires substantially increased brightness which is predicted to be achievable using plasma—vacuum interfaces as the nonlinear medium for the conversion of few-cycle optical pulses into attosecond pulses [9].

Solid density targets can result in nearly steplike plasma—vacuum interfaces—plasma mirrors—when irradiated with a high-contrast laser pulse. Two distinct nonlinear conversion processes contribute to the harmonic emission from plasma mirrors: coherent wake emission (CWE) [10–12] and the relativistically oscillating mirror (ROM) [13–16]. The ROM process can be understood in terms of the relativistic motion of the apparent reflection point, and thus ROM harmonics become dominant when the normalized vector potential a_L, which in terms of the focused laser intensity I_L is given by $a_L^2 = I_L \lambda_L^2/(1.38 \times 10^{18}\ \mathrm{W\,cm^{-2}}\ \mu\mathrm{m}^2)$, is significantly larger than unity, while for $a_L \lesssim 1$ the CWE mechanism is considerably more efficient. While attosecond pulse trains generated using the CWE process have been experimentally observed [17,18], they have been significantly above the transform limited pulse duration. ROM harmonics by contrast possess superior phase characteristics and are therefore better suited to the generation of isolated attosecond pulses with near transform limited pulse durations [19]. Additionally, ROM has higher efficiency in the relativistic limit $a_L \gg 1$ [20] and extends to far higher photon energies [21].

Here, we study the nonlinear behavior of ROM harmonics in the few-cycle limit for the first time and investigate their suitability for the generation of intense isolated attosecond pulses [9]. A detailed numerical investigation by particle-in-cell simulations reveals that carrier envelope (CE)-stabilized three-cycle pulses are already sufficient for the production of isolated attosecond pulses. In agreement with theoretical predictions, we observe the onset of supercontinuum generation experimentally, the essential prerequisite for isolated attosecond pulses. To our knowledge, this is also the first observation of ROM harmonics generated with an optical parametric chirped-pulse amplification system, the LWS-20, highlighting the unrivalled potential of this technology for the generation of powerful few-cycle pulses [22,23].

In general, any process that produces a broad spectrum with well-defined spectral phase has the potential to generate attosecond pulses. In the particular case of femtosecond-duration optical lasers, the effective bandwidth is dramatically increased by generating a large number of high-order harmonics via a suitable nonlinear

conversion mechanism (e.g., noble-gas atoms, ROM, or CWE). Since the nonlinear processes are generally strongly intensity dependent, the harmonic conversion is temporally localized to times of high instantaneous intensity, i.e., once per (half-) cycle for ROM (for gaseous media). Thus one would expect to see each burst of harmonic generation to lead to the emission of a distinct attosecond pulse and hence in general the production of an attosecond pulse train. Producing an isolated pulse therefore requires significant harmonic production to be restricted to one (half-) cycle. The relative strength of individual attosecond bursts depends on the effective nonlinearity of the process and the peak intensity of each (half-) cycle. The most energy efficient way of achieving an isolated attosecond pulse is thus to exploit the rapidly varying intensity of a few-cycle laser pulse, whereby the larger temporal separation of one full optical cycle between individual attosecond bursts for ROM harmonics will contribute to relaxing the constraints on the maximum pulse duration, which still produces an isolated attosecond pulse. Clearly, CE phase critically affects the relative intensity of adjacent (half-) cycles and, hence, the pulse duration required to produce an isolated attosecond pulse. The question that arises is how short the laser pulse needs to be to produce isolated pulses independently of the CE phase and what pulse duration can deliver similar performance in the presence of CE stabilization. Naively, one would assume that choosing a CE phase of $\varphi = 0$ (corresponding to a cosine pulse, i.e., the peak of E field coincides with the peak of the envelope) would be the best solution.

To address the questions raised above, we have performed a systematic numerical study in which the CE phase was varied between $\varphi = 0$ and $\varphi = 2\pi$ while all other input parameters were kept constant. The 1D PIC simulation parameters were chosen to closely match those currently experimentally obtainable. Studies were performed at a pulse duration of 8 fs (corresponding to 3 cycles full width half maximum (FWHM) in intensity, which is currently the shortest pulse duration for multiple-terawatt lasers capable of reaching the relativistic regime of $a_L > 1$) and 5 fs, which corresponds to the future performance of the LWS laser. The laser was set to an average $a_L = 2.0$ with an angle of incidence of $\Theta_L = 45°$ and an electron density n_e in units of the critical density n_c of $n_e \approx 400$ (corresponding to the fused silica targets) with an exponential density ramp with a scale length of $L = \lambda_L/8$. The reflected waveforms were analyzed with a particular emphasis on the resulting attosecond pulse train. The analysis procedure is elucidated in Fig. 1 for two values of CE phase for otherwise identical conditions. The harmonic spectrum for each value of CE phase is obtained through fast Fourier transform of the E field after reflection by the plasma medium [Figs. 1(a) and 1(d)]. The spectrum is multiplied by a numerical filter chosen to correspond to the spectral observation window of the associated experiment [see dotted line in Figs. 1(b) and 1(e)]. An inverse fast Fourier transform of the filtered spectrum then yields the temporal structure of the attosecond pulse train [Figs. 1(c) and 1(f)]. The distortion of the electric field waveform that gives rise to the harmonic spectrum is clearly evident. The high nonlinearity of the process, both in terms of efficiency slope and cutoff frequency result in the emission of an attosecond pulse only for the three strongest cycles within the pulse. Comparing the respective emission time of the attosecond pulses in Figs. 1(c) and 1(f) with the reflected waveform, one can see that, as expected, the attosecond pulses are temporally localized at the points where the slope of the reflected waveform is steepest. The duration of the attosecond pulse train envelope was obtained by performing a least-squares Gaussian fit $I_{\text{train}}(t) \propto \exp(-4\ln 2 t^2/\tau_{\text{train}}^2)$ to the attosecond pulses [in Figs. 1(c) and 1(f)]. In addition, we adopt quite arbitrarily the criterion that the number of attosecond pulses in the train is given by the number of pulses with an intensity higher than $1/e^2$ of the main attosecond pulse intensity [dotted line in Figs. 1(c) and 1(f)]. This yields a measure of the duration of the attosecond pulse train τ_{train} and of the number of attosecond pulses $N_{\text{as-pulse}}$ in it.

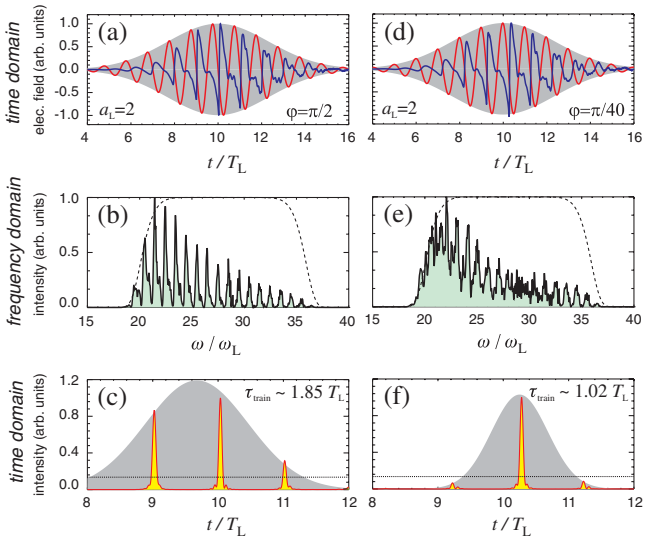

FIG. 1 (color). 1D PIC simulation of the laser-plasma interaction using the code LPIC [14]. (a) and (d): E fields of incident (red) and reflected (blue) three-cycle laser pulses for a CE phases of $\varphi = \pi/2$ and $\varphi = \pi/40$. (b) and (e): Spectra obtained by fast Fourier transform of the E fields after spectral selection by the filter shown as dotted line. (c) and (f): Time domain behavior of the filtered spectra. Note the appearance of the attosecond pulses at the points of the steepest slopes in the individual cycles. The intensity of the attosecond pulses that comprise the attosecond pulse train is in red. The gray Gaussian curve is a fit to the attosecond pulse train to quantitatively deduce its width. The dashed line corresponds to $1/e^2$ of the strongest attosecond pulse.

According to our criterion, the examples in Fig. 1 clearly show that for a laser pulse with $\tau_L = 3T_L$, where T_L is the duration of a single cycle, depending on the CE phase the resulting attosecond pulse train can consist of three ($\varphi = \pi/2$) or one ($\varphi = \pi/40$) individual attosecond pulse. Note that for the individual attosecond pulse the harmonics are beginning to merge and form a spectral quasi-continuum, characteristic of an isolated attosecond pulse.

The temporal structure of the attosecond trains produced by a three-cycle laser pulse for all values of φ between 0 and 2π is summarized in Fig. 2. The relative intensity and emission time is shown in Fig. 2(a) with the relative intensity color-coded on a logarithmic scale. The FWHM duration of the attosecond train τ_{train} is given vs CE phase in Fig. 2(b). The nonlinearity of the process results in a CE-phase-dependent reduction of the pulse-train envelope to between 1 and 2 T_L, with up to four individual attosecond pulses above the $1/e^2$ threshold. As expected, the emission time of the dominant attosecond pulse shifts according to the CE phase of the laser pulse envelope. For a CE phase of $\varphi \simeq 4.71$ rad, isolated attosecond pulses are reliably produced over a window of $\Delta\varphi = \pm 0.31$ rad. It is interesting to note that the average width of the train is $\langle \tau_{train}/T_L \rangle = 1.47 \pm 0.4$. The degree of the instantaneous nonlinearity α of the process defined as $I_{train}(t) \sim I_L^{\alpha}(t)$ is estimated as $\alpha \simeq \langle (\tau_L/\tau_{train})^2 \rangle = 5.0 \pm 2.3$. Assuming no phase stabilization, i.e., φ as random, we can evaluate the percentage of the shots that produce isolated attosecond pulses. For a three-cycle laser pulse, we obtain a 17% likelihood to produce an isolated attosecond pulse (with 29% resulting in double, 49% resulting in triple, and 5% resulting in quadruple pulse trains). Performing a similar analysis using a two-cycle pulse (5.3 fs) increases the probability of producing an isolated attosecond pulse to 50%, making it reasonable to perform experiments with isolated attosecond pulses using only CE tagging of individual laser pulses and thus removing the need for CE stabilization of the laser.

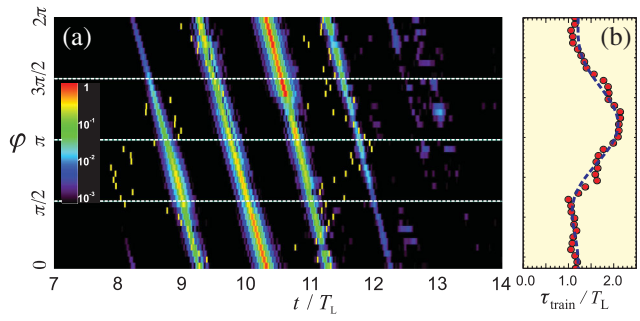

FIG. 2 (color). Variation of the number of attosecond pulses with the CE phase of the laser pulse. (a) The color-coded plot shows in logarithmic scale the train of attosecond pulses as a function of time of occurrence for values of $\varphi = 0$ to 2π. The yellow bars for each value of φ indicate the region outside which the satellite pulses are less than $1/e^2$ of the main pulse. (b) Variation of the pulse train width (FWHM) with φ (points from simulation data, dashed line from fit to the data).

As can be seen from Fig. 1, the variation in the spectral structure for different values of CE phase with otherwise identical conditions is very substantial and should therefore be easily observable experimentally. The experiment was performed under conditions that matched the simulations as closely as possible. The p-polarized laser was focused using an $f/3$, 30° off-axis parabola onto the fused silica target at $\Theta_L = 45°$. With a pulse energy of ≈ 60 mJ on target, this yields an averaged, normalized vector potential inside the first Airy minimum of $a_L \approx 2.0$. The peak intensity is estimated to be $a_L^{peak} \approx 3$. The scale length was assessed as $L = \lambda_L/8$, based on an approximate plasma expansion velocity of 10^7 cm/s and an expansion time interval of ≈ 1 ps before the peak of the laser pulse, i.e., the point where plasma is estimated to be generated. The emitted harmonic radiation in the specular direction was collected by a 3 in. spherical mirror with unprotected gold coating at 70° angle of incidence and then directed onto the entrance slit of a grazing-incidence imaging extreme ultraviolet spectrometer equipped with a 150 nm Al filter. Figure 3(a) shows a typical harmonic spectrum together with a raw image of the spectrometer. The spectra contain harmonic radiation well above the CWE cutoff at harmonic 20 (H20) and extending close to the Al filter cutoff at 17 nm. The effect of the shortness of the laser pulse on the harmonic spectrum becomes evident in the comparison

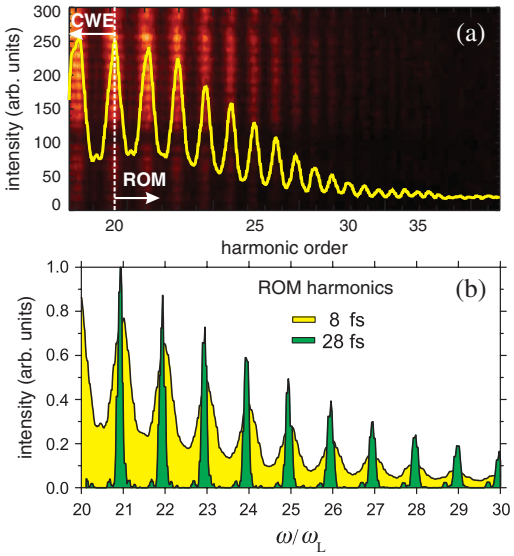

FIG. 3 (color). (a) Single-shot raw data of the emitted harmonic radiation. The spectrum (yellow line) is obtained after vertical binning of the record. The horizontal structure is due to the supporting mesh of the Al filter. (b) Recorded spectra in the frequency domain with laser pulses of different duration but comparable laser pulse intensity on target and central wavelength of $\lambda_L = 815$ nm; in yellow with a pulse duration of $\tau_L = 3T_L \sim 8$ fs and in green with a pulse duration of $\tau_L = 10T_L \sim 28$ fs (see Ref. [24]).

of two spectra obtained under similar conditions but one with a three-cycle and the other with a 10-cycle laser pulse from another laser system [24]. As seen in Fig. 3(b), there is a dramatic increase in the bandwidth of the harmonics resulting in partial overlap, and the spectrum now forms a modulated continuum, which is the prerequisite for an isolated attosecond pulse.

A series of eight single-shot, background-corrected spectra of the reflected radiation in the H20-H35 spectral range acquired under nominally the same experimental conditions is shown in Fig. 4. Despite the fact that all the accessible laser parameters were kept constant, substantial shot-to-shot variation of the spectral structure is observable. Although no one-to-one correspondence between experimental and calculated spectra can be made since the CE phase of the laser pulse was not measured, it is possible to find simulated spectra with a striking similarity to the features observed in the experiment. For example, the smooth spectrum in Fig. 1(b), which corresponds to a triple pulse train, is remarkably similar to the spectra in Figs. 4(b) and 4(e) whereas the structured spectrum in Fig. 1(e) corresponding to a single, isolated attosecond pulse matches the experimental spectra in Fig. 4(f) and 4(g) very well. The shot-to-shot variation of the spectral structure is attributable to the random fluctuation of the unstabilized carrier-envelope phase of the driving laser pulse. This interpretation is consistent with our simulation data (Fig. 1), which highlights how small variations in the relative intensities and positions of the attosecond pulses in the temporal domain manifest themselves in significant changes in the spectral domain. In contrast, fluctuations of other parameters such as pulse duration and energy are very small ($< 5\%$) and insufficient to account for the observed variability. Inducing comparable change in the spectrum requires very substantial change in the interaction conditions, such as deliberate and substantial changes to the pulse contrast as shown for multicycle pulses (where CE effects are negligible) by Behmke *et al.* [25]. However, the explanation furnished in that case is not applicable to our measurements because the laser pulse contrast was kept constant at the highest possible level of 10^8 at 2 ps and $>5 \times 10^9$ at 20 ps before the pulse peak by using a cross-polarized wave generation unit. Our interpretation of the spectral signatures is supported by the average spectral width of the observed harmonics $\langle \Delta\omega/\omega_L \rangle = 0.45 \pm 0.017$, which is significantly broader than the Fourier-transform limited value of the laser envelope $\Delta\omega/\omega_L = 0.44 T_L/\tau_L \approx 0.15$. The implied temporal duration of the attosecond pulse-train envelope and nonlinearity of the generation process are also in very good agreement with the simulations. Note that the pulse duration at which a single attosecond pulse is obtained for ROM process is less stringent than that for the atomic medium [4]. This is primarily due to the fact that whereas an attosecond pulse is generated twice per optical cycle in the case of the atomic medium, ROM harmonics at oblique incidence are only emitted once per cycle, effectively reducing the number of attosecond pulses generated under an envelope of given width and thus allowing single attosecond pulses to be achieved with longer drive pulses. Alternatively, for sufficiently short laser pulses, a more intense part of the spectrum can be selected at lower harmonics without the need to use cut-off harmonics only.

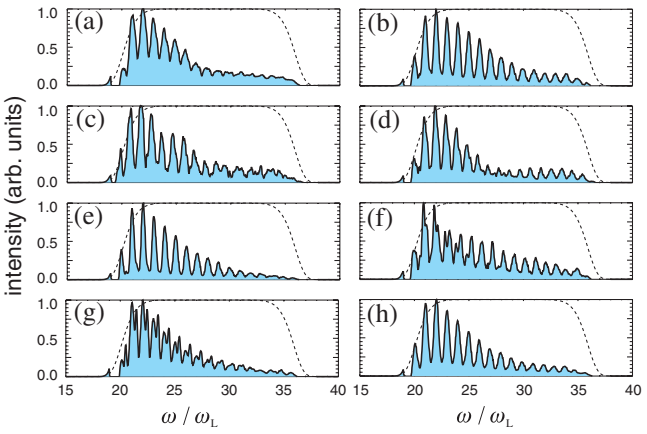

FIG. 4 (color). Sample recorded spectra in the frequency domain after background subtraction acquired with random carrier-envelope phase but otherwise identical experimental conditions, i.e., with 60 mJ laser pulse energy on target, a pulse duration of $\tau_L = 3T_L \sim 8$ fs, and a central wavelength of $\lambda_L = 815$ nm.

In conclusion, we have experimentally shown that in the limit of few-cycle pulses, ROM harmonics driven by a 16 TW laser exhibit broad harmonic peaks resulting in partial overlap and continuous spectral content. This conforms to the results of PIC simulations, which show that using three-cycle pulses (8 fs) as many as 17% of the shots with random CE phase give rise to a single dominant attosecond pulse. For the current laser performance, CE-phase stabilization or CE-phase tagging would already allow intense single attosecond pulses to be generated for both pumping and probing. The current analysis shows that a further reduction in pulse duration to two cycles (5.3 fs) results in a probability of $\geq 50\%$ for isolated attosecond pulses to be generated, thus greatly relaxing the requirements for precise CE-phase stabilization. The combination of the high conversion efficiencies of the ROM process and the ability to efficiently harness petawatt-class high energy lasers thus paves the road to attosecond pulses of unprecedented intensity.

The authors would like to thank B. Dromey for reading the manuscript and making useful suggestions. This work was funded in part by the DFG Project No. TR-18 and the MAP excellence cluster, by Laserlab-Europe, Grant No. 228334, and by the association EURATOM-MPI für Plasmaphysik. J. M. M. gratefully acknowledges financial support from the Alexander-von-Humboldt Foundation and RFBR Grants No. 08-02-01245-a and No. 08-02-01137-a.

*Corresponding author: info@patrick-heissler.de

[1] A. Baltuska, M. Uiberacker, E. Goulielmakis, R. Kienberger, V. S. Yakovlev, T. Udem, T. W. Hänsch, and F. Krausz, IEEE J. Sel. Top. Quantum Electron. **9**, 972 (2003).
[2] M. Hentschel, R. Kienberger, C. Spielmann, G. A. Reider, N. Milosevic, T. Brabec, P. Corkum, U. Heinzmann, M. Drescher, and F. Krausz, Nature (London) **414**, 509 (2001).
[3] A. Baltuska, T. Udem, M. Uiberacker, M. Hentschel, E. Goulielmakis, C. Gohle, R. Holzwarth, V. S. Yakovlev, A. Scrinzi, T. W. Hänsch, and F. Krausz, Nature (London) **421**, 611 (2003).
[4] E. Goulielmakis, M. Schultze, M. Hofstetter, V. Yakovlev, J. Gagnon, M. Uiberacker, A. L. Aquila, E. M. Gullikson, D. T. Attwood, R. Kienberger, F. Krausz, and U. Kleineberg, Science **320**, 1614 (2008).
[5] G. Sansone, E. Benedetti, F. Calegari, C. Vozzi, L. Avaldi, R. Flammini, L. Poletto, P. Villoresi, C. Altucci, R. Velotta, S. Stagira, S. De Silvestri, and M. Nisoli, Science **314**, 443 (2006).
[6] M. Uiberacker, T. Uphues, M. Schultze, A. J. Verhoef, V. S. Yakovlev, M. F. Kling, J. Rauschenberger, M. N. Kabachnik, H. Schröder, M. Lezius, K. L. Kompa, H.-G. Muller, M. J. J. Vrakking, S. Hendel, U. Kleineberg, U. Heinzmann, M. Drescher, and F. Krausz, Nature (London) **446**, 627 (2007).
[7] A. L. Cavalieri, N. Müller, T. Uphues, V. S. Yakovlev, A. Baltuska, B. Horvath, B. Schmidt, L. Blümel, R. Holzwarth, S. Hendel, M. Drescher, U. Kleineberg, P. M. Eschenique, R. Kienberger, F. Krausz, and U. Heinzmann, Nature (London) **449**, 1029 (2007).
[8] P. Tzallas, E. Skantzakis, L. A. A. Nikolopoulos, G. D. Tsakiris, and D. Charalambidis, Nature Phys. **7**, 781 (2011).
[9] G. D. Tsakiris, K. Eidmann, J. Meyer-ter Vehn, and F. Krausz, New J. Phys. **8**, 19 (2006).
[10] F. Quéré, C. Thaury, P. Monot, S. Dobosz, P. Martin, J.-P. Geindre, and P. Audebert, Phys. Rev. Lett. **96**, 125004 (2006).
[11] C. Thaury, F. Quéré, J.-P. Geindre, A. Levy, T. Ceccotti, P. Monot, M. Bougeard, F. Rau, P. d'Oliveira, P. Audebert, R. Marjoribanks, and P. Martin, Nature Phys. **3**, 424 (2007).
[12] P. Heissler, R. Hörlein, M. Stafe, J. Mikhailova, Y. Nomura, D. Herrmann, R. Tautz, S. Rykovanov, I. Földes, K. Varjú, F. Tavella, A. Marcinkevicius, F. Krausz, L. Veisz, and G. Tsakiris, Appl. Phys. B **101**, 511 (2010).
[13] P. Gibbon, Phys. Rev. Lett. **76**, 50 (1996).
[14] R. Lichters, J. Meyer-ter Vehn, and A. Pukhov, Phys. Plasmas **3**, 3425 (1996).
[15] T. Baeva, S. Gordienko, and A. Pukhov, Phys. Rev. E **74**, 046404 (2006).
[16] B. Dromey, D. Adams, R. Hörlein, Y. Nomura, S. G. Rykovanov, D. C. Caroll, P. S. Foster, S. Kar, K. Markey, P. McKenna, D. Neely, M. Geissler, G. D. Tsakiris, and M. Zepf, Nature Phys. **5**, 146 (2009).
[17] Y. Nomura, R. Hörlein, P. Tzallas, B. Dromey, S. Rykovanov, Z. Major, J. Osterhoff, S. Karsch, L. Veisz, M. Zepf, D. Charalambidis, F. Krausz, and G. D. Tsakiris, Nature Phys. **5**, 124 (2008).
[18] R. Hörlein, Y. Nomura, P. Tzallas, S. Rykovanov, B. Dromey, J. Osterhoff, Z. Major, S. Karsch, L. Veisz, M. Zepf, D. Charalambidis, F. Krausz, and G. D. Tsakiris, New J. Phys. **12**, 043020 (2010).
[19] S. Gordienko, A. Pukhov, O. Shorokhov, and T. Baeva, Phys. Rev. Lett. **93**, 115002 (2004).
[20] B. Dromey, M. Zepf, A. Gopal, K. Lancaster, M. S. Wei, K. Krushelnick, M. Tatarakis, N. Vakakis, S. Moustaizis, R. Kodama, M. Tampo, C. Stoeckl, R. Clarke, H. Habara, D. Neely, S. Karsch, and P. Norreys, Nature Phys. **2**, 456 (2006).
[21] B. Dromey, S. Kar, C. Bellei, D. C. Carroll, R. J. Clarke, J. S. Green, S. Kneip, K. Markey, S. R. Nagel, P. T. Simpson, L. Willingale, P. McKenna, D. Neely, Z. Najmudin, K. Krushelnick, P. A. Norreys, and M. Zepf, Phys. Rev. Lett. **99**, 085001 (2007).
[22] T. H. Dou, R. Tautz, X. Gu, G. Marcus, T. Feurer, F. Krausz, and L. Veisz, Opt. Express **18**, 27900 (2010).
[23] D. Herrmann, L. Veisz, R. Tautz, F. Tavella, K. Schmid, V. Pervak, and F. Krausz, Opt. Lett. **34**, 2459 (2009).
[24] L. Waldecker, P. Heissler, R. Horlein, K. Allinger, M. Heigoldt, K. Khrennikov, J. Wenz, S. Karsch, F. Krausz, and G. Tsakiris, Plasma Phys. Controlled Fusion **53**, 124021 (2011).
[25] M. Behmke, D. an der Brügge, C. Rödel, M. Cerchez, D. Hemmers, M. Heyer, O. Jäckel, M. Kübel, G. G. Paulus, G. Pretzler, A. Pukhov, M. Toncian, T. Toncian, and O. Willi, Phys. Rev. Lett. **106**, 185002 (2011).